MEASUREMENT OF CHARGE EMISSION FROM TARGETS AS A MEANS OF

BURST INTENSITY AND BEAM INTENSITY MONITORING

K. Budal

European Organization for Nuclear Research
Geneva, Switzerland

Summary

Internal and external operational targets for the CERN Proton Synchrotron have been electrically insulated and the charge emission from the targets measured as a means of burst intensity monitoring. Charge emission from plates placed in ejected beams have been used for beam intensity monitoring. The measurements presented here concern linearity, saturation and reproduceability tests and investigations of the various parameters influencing the signal level. The main contribution to the signal comes from δ-rays which escape from the target. Theoretical results are presented and compared with experimental results.

Experimental Results (1-4)

Method of Measurement

Most of the measurements were performed as shown in Fig. 1. The target is electrically insulated and connected to a coaxial cable which leads to an integrating electrometer (5) in the Main Control Room. The electrometer consists of an integrating capacitor C, two gated relays, G and R, and a high input impedence amplifier, A. During the targeting period, gate G is closed. Hence the charge removed from the target is stored on the condenser. After the signal is registered on the scaler, the relay R short-circuits the condenser, making the instrument ready for the next burst.

Internal Targets

The signal from a 1^p x 20 mm Be target was measured with respect to the beam intensity and to the signal from the standard telescope target monitor (6). The latter is placed in a separate beam channel, 30 m from the target and counts particles at a production angle of $45°$. Measuring results are shown in Fig. 2.

Table I shows how the same ratios change for different burst widths. The charge and telescope measurements agree excellently, except for the case when the beam was bunched. A bunched beam gives a series of extremely short bursts which is expected to give saturation effects in the telescope counter due to its finite time resolution. The last column shows how the target efficiency changes with targeting conditions.

Measurement of charge transport from operational Be targets 1^p x 20 mm were made at

intervals throughout 1966 under, as far as possible, the same conditions. Variations in signal level were maximum 7%. The difference between the signal from top and bottom targets in the same experiment amounted to 1 - 2%. The long-term variations may be due to drift in beam current monitors or uncontrollable changes in targeting conditions.

Table II shows the signal levels from targets of different materials and shapes, as a function of proton momentum. There is a big change in target efficiency by momentum, as is evident from the theoretical values (7) given in line B. Plate efficiencies represent rough estimates only. Correcting for the different target efficiencies, we obtain the signal for 100% target efficiency (A/B) (the number of elementary charges ejected per interaction), which gives the best basis for comparison.

An idea of the low-energy component of the charge transport from targets is obtained by applying a bias voltage. Fig. 3 shows how the signal level changes as a function of bias voltage for a 1^p x 20 mm Be target. The small change for the positive bias is most likely an effect of the finite insulation resistance of the target system.

External Wire Targets

External targets are placed in air. This introduces the difficulty that as soon as a voltage is established on the target, free charges are collected from the heavily ionized air and partly neutralize the signal. This problem was partly overcome by coating the target with a thin insulating layer of aluminium oxide. The emission of the high-energy particles (mainly δ-rays) is only influenced in so far as the target dimensions are changed, whereas the low-energy, free air charges are prevented from entering. (The capacitively induced charge is negligible.)

An experiment was made with a coated target and it was found that the charge collection from air was reduced by a factor of 4 as compared to the uncoated case. The effect amounted to ca. 0.7% signal change per volt bias voltage. This is still somewhat large. There is probably room for improvement.

The linearity of a coated Cu target, 1 x 2 x 150 mm, was measured with respect to ejected beam intensity during fast ejection. Fig. 4 shows the results of a measurement with a particularly stable beam. The integrating

capacitor was in this case 0.49 µF and the amplification was 5. This gives a signal level of 3.1 C per 10^{11} ejected protons, or 1.9 electrons per ejected proton. Only a fraction of the protons interact in the target.

The charge emission is a function of distribution of interactions in the target. This is clearly seen from Fig. 5, which shows how the signal changes as a 4 x 4 x 150 mm Cu target is moved across a ≈2.5 x 1 mm beam (H x V) in the vertical direction. The depth of the valley was found to be much smaller for a 2 x 2 mm target (8) and not even observable for a 1 x 2 mm target.

Plates in Ejected Beams

Plate targets are occasionally used for intensity monitoring of ejected beams. The plates are placed in the television screen exchangers (9) in such a way that they can be easily moved in and out of the beam. The screen exchanger units are evacuated, eliminating the problem of ionized air.

The plate signal was measured with respect to ejected beam current and was found to be linear. Charge emission efficiency was found, within experimental errors ($\pm$ 5%), to be the same for fast and slow ejection, which indicates that no saturation effects are present. No momentum dependence was found. Several Al plates with the same thickness and tilting angle were tested and found to have the same ($\pm$ 5%) charge emission efficiency.

The signal levels from Al plates of various thicknesses and two different tilting angles were measured. Results are given in Table III. The efficiency is given in number of elementary charges ejected per penetrating proton.

Fig. 6 shows how the signal from the 0.5 mm plate at 15° was influenced by an applied bias voltage.

Interpretation of Experimental Results

Figs. 3 and 6 show that the signal from insulated targets can be influenced to some extent by applying a bias voltage. Part of the observed effect arises from the finite insulation resistance of the target system. Most of the change, however, is due to a low-energy particle component which can be controlled by a bias voltage. This component is probably electrons in the range 0-50 eV, responsible for the signal in secondary emission monitors (9).

The main contribution to the signal is believed to come from escaped knock-on electrons (10). The large signal dependence on material and shape (Table II) and distribution of interactions (Fig. 5) are δ-ray absorbtion effects. A magnetic field may turn ejected δ-rays back to the target. This explains the seemingly large momentum dependence for plates (Table II).

The important parameter in this respect is the target height in the field direction.

A third contribution to the charge transport comes from shower particles. Take as an example a proton-proton interaction. If none of the interaction products are absorbed, obviously one elementary charge is removed from the target per interaction. Spallation products may also be able to escape. Pair production, photo-emission and Compton scattering may be mentioned as well as possible charge emission mechanisms.

Theoretical Results (11)

A method, based on Monte Carlo calculations, has been worked out for finding the charge emission efficiency of targets. Computer programs have been made for circular, rectangular and plate targets. Input parameters are: target material and dimensions, tilting angle with respect to beam direction, distribution of interactions in the target and the magnetic field strength at the target position. Two charge ejection mechanisms have been considered, namely: δ-ray ejection due to the primary proton beam and the charge carried away by the shower particles. For the latter we have assumed that one positive charge is removed from the target per interaction. In the case of the plate target also, the δ-ray ejection due to the charged shower particles have been taken into account. The low-energy electron component is not considered. This component may be controlled by a bias voltage or eliminated by coating the target surface.

Fig. 7 shows the computed charge emission efficiency for beryllium wire targets as a function of target dimensions. The distribution of interactions is taken to be uniform throughout the target cross section. Parameters are tilting angle of target and magnetic field strength at target position. The efficiency is given in number of elementary charges ejected from the target per interaction. By interaction, the total number of primary and secondary, elastic and inelastic collisions is meant here.

Fig. 8 demonstrates the variation in charge emission efficiency for different parts of the target. The case considered is that the interactions take place within a small area with dimensions 0.2 x height and 0.1 x width of the target. The curve shows the efficiency as a function of the position of the area. This will roughly correspond to the case of a thin beam pencil moving across the target. (For thick targets, secondary interactions change the distribution significantly.)

Fig. 9 gives the number of elementary charges emitted from aluminium plates per penetrating proton, as a function of plate thickness and tilting angle.

Comparison Between Theory and Experiment

The 1^{ϕ} x 20 mm Be targets are the ones most extensively tested. The distribution of inter-actions in thin internal wire targets is closely uniform (12). Hence, from Fig. 7, we obtain the charge emission efficiency, 18.5. Since the target is thin, this is nearly equal to the number of primary proton interactions. Taking the case of a long burst at the flat top (Table I, Fig. 2), the experimental value is 13.7, giving a target efficiency of 13.7/18.5 = 0.74. A direct measurement (13) indicates a value ca. 0.60, whereas the theoretical value (line B, Table II) is somewhat higher, namely 0.78.

For the 3 x 2 x 38 mm Be target, we have one measurement only, in which we obtained the efficiency (see Table II and Fig. 7), 5.4/9.6 = 0.56. The theoretical value (Table II) is 0.75, considerably higher.

In Fig. 10, we have plotted the experimental plate efficiencies against the computed ones (Fig. 9). The error limits shown are partly due to uncertainties in the measurements of the charge transport and partly due to uncertainties in the tilting angle ($\pm$ 0.5°). The points fit reasonably well into a straight line which can be expressed by the equation

$$\text{Exp.} - 0.015 = 0.90 \ E_{Th}$$

The constant 0.015 is interpreted as the low-energy signal component (see Fig. 6). Its value is somewhat lower than obtained from Fig. 6, but in this experiment we had the additional effect of leakage currents. Moreover, it is assumed that the number of low-energy electrons ejected per proton traversal is independent of the tilting angle. This may not be the case. The coefficient 0.90 means that the beam intensity as measured with the plates (used as absolute monitors) is only ca. 90% of that measured with the beam current transformer.

It seems that the greater part of the observed charge transport from targets and plates can be explained in terms of δ-ray and shower particle emission.

References

1. K. Budal, CERN internal report MPS/CO 66-5

2. K. Budal and Ch. Serre, CERN internal report MPS/CO 66-29

3. V. Agoritsas et al, CERN internal note MPS/MU-Note/EP 66-41

4. D. Dekkers, L. Henny and L. Hoffman, CERN internal note MPS/MU-Note/EP 66-42

5. V. Agoritsas and J.J. Merminod, "Electrometer Amplifier and Digitizer". To be published in Nucl. Instr. and Methods

6. V. Agoritsas, B. Bonaudi, CERN internal note MPS/ALO 62-8

7. H.G. Hereward, J. Ranft and W. Richter, "Efficiency of Multi Traversal Targets" CERN yellow report 65-1

8. H. van der Beken and Ch. Serre, private communication

9. V. Agoritsas et al, report in these proceedings

10. Also observed to be ejected from the foils of secondary emission chamber; see R.A. Shatas, J.F. Marshall and M.A. Pommerantz, Phys. Rev. 96, 1199 (1954); B. Planskoy, Nucl. Instr. and Meth. 24 (1963), 172; S.A. Blankenberg, J.K. Cobb and J.J. Murray, SLAC-PUB 107 (1965)

11. A more detailed report is in preparation

12. J. Ranft, private communication; see also Ref. 7

13. A. Colombo, private communication

Burst (ms)	Target/telescope (relative units)	Target/beam int. (el./circ.prot.)
150	111	13.7
100 (servo)	113	13.3
25	110	14.0
0.15 (debunched)	112	12.6
0.15 (bunched)	143	5.27
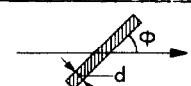
Table I

d (mm)	0.05	0.5	1.0	3.0	0.05	0.5
ϕ	29.5°	29.5°	29.5°	29.5°	15°	15°
Efficiency (el./prot.)	0.042	0.078	0.097	0.118	0.065	0.138

Table III

Table II

Material	Al			Al			Cu			Be			Be +		Be
Dimension	1 mm plate			5 mm plate			1 mm plate			1$^\phi$x20 mm			1$^\phi$x20 mm		3x2 mm
Position															
Momentum (GeV/c)	19.2	15.	10.	19.2	15.	10	19.2	15.	10.	19.2	15.	10.	19.2	10.	21.66
(A) Signal (el./circ. proton)	4.0	3.7	2.8	1.7	1.6	1.3	1.1	1.0	0.74	11.9	9.9	7.8	13.0	8.6	5.4
(B) Target efficiency (7)	0.54	0.42	0.27	0.54	0.42	0.27	0.35	0.27	0.16	0.78	0.66	0.47	0.78	0.47	0.75*
(A/B) Signal for 100% target efficiency	7.4	8.8	10.4	3.2	3.8	4.8	3.1	3.7	4.6	15.3	15.0	16.6	16.7	18.3	7.2
Magn.stray field (kG)	2.2	1.7	1.1	2.2	1.7	1.1	2.2	1.7	1.1	2.0	1.5	1.0	2.4	1.2	2.2

* Beam steering to inside   + Different position
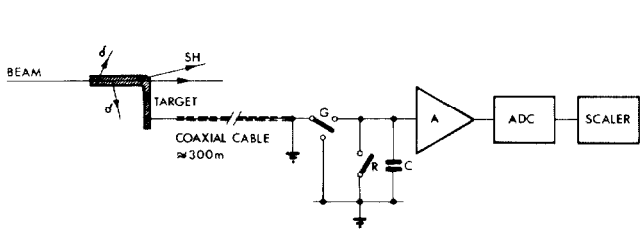
Fig. 1. Principle of measurement.
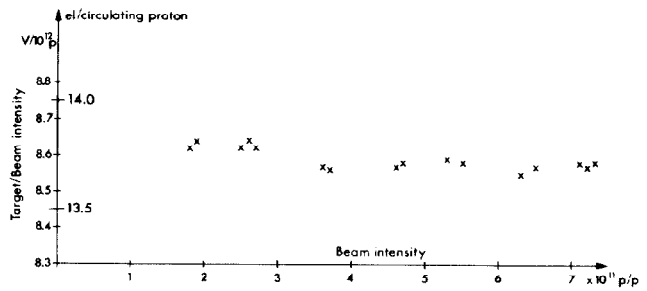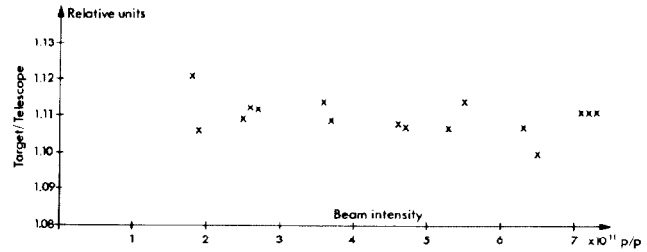
Fig. 2. Linearity test. Internal Be target,
1$^\phi$ × 20 mm.
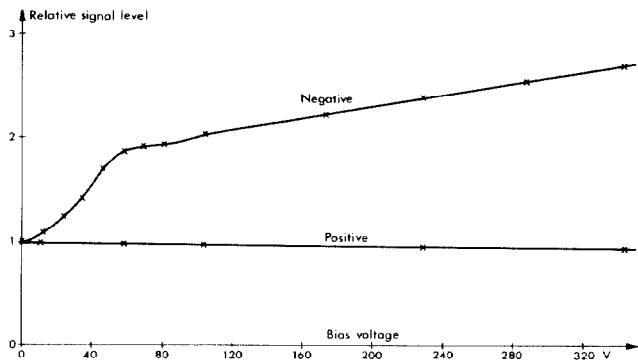
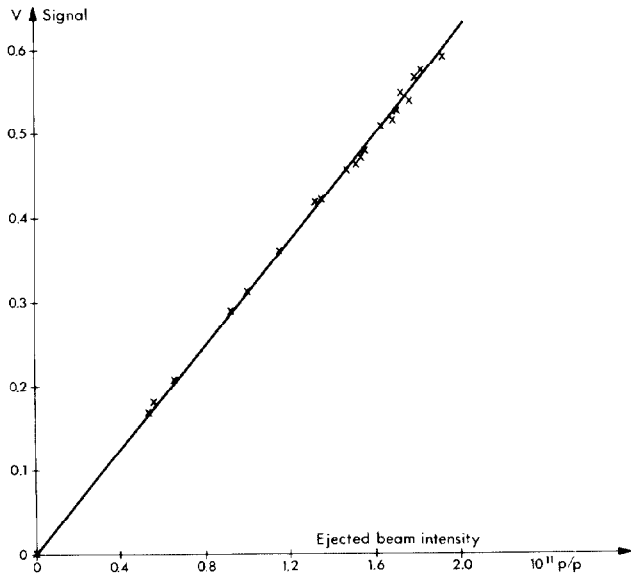Fig. 3. Influence of bias voltage on charge transport
from internal Be target, 1$^\phi$ × 20 mm.

Fig. 4. Linearity test. Coated Cu target, 2 × 1
× 150 mm.
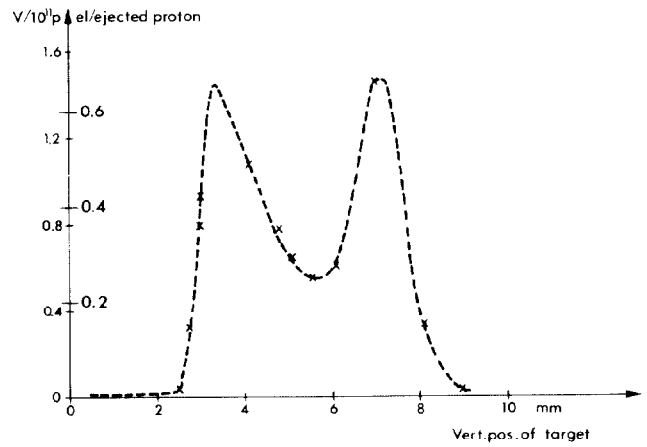

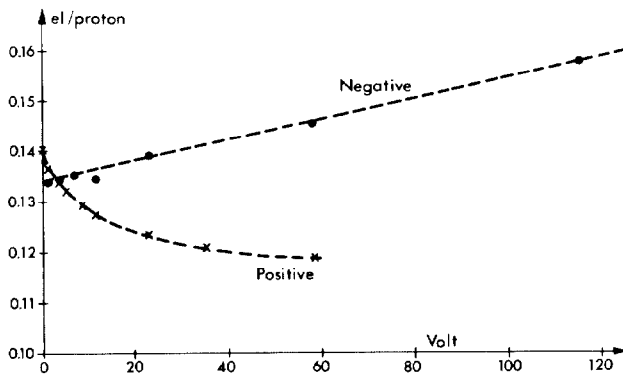Fig. 5. A 4 × 4 mm Cu target is moved across
a ≈ 2.5 × 1 mm beam.

Fig. 6. Influence of bias voltage on charge transport
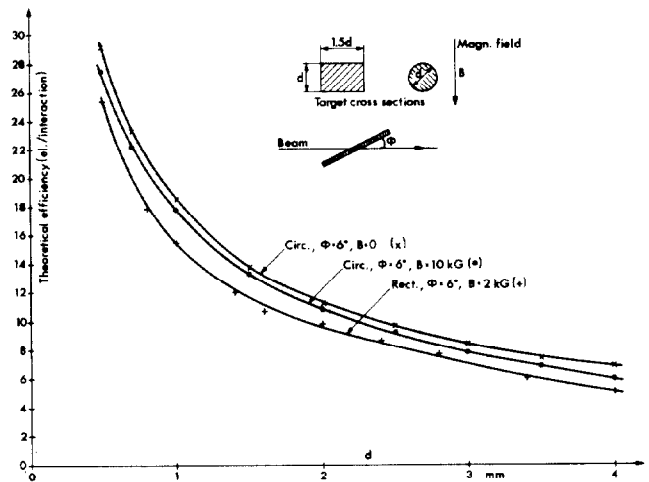from insulated Al plate, 0.5 mm, 15°.

Fig. 7. Theoretical charge emission efficiency of Be
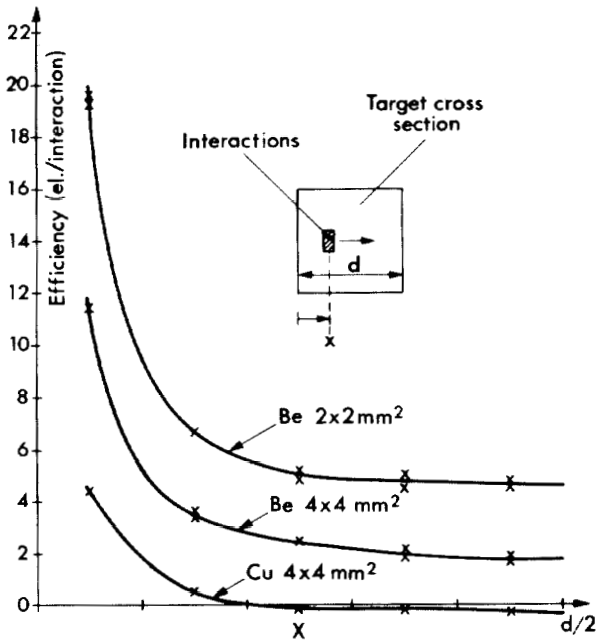wire targets as a function of target
dimensions.

Fig. 8. Theoretical charge emission efficiency for different parts of target.
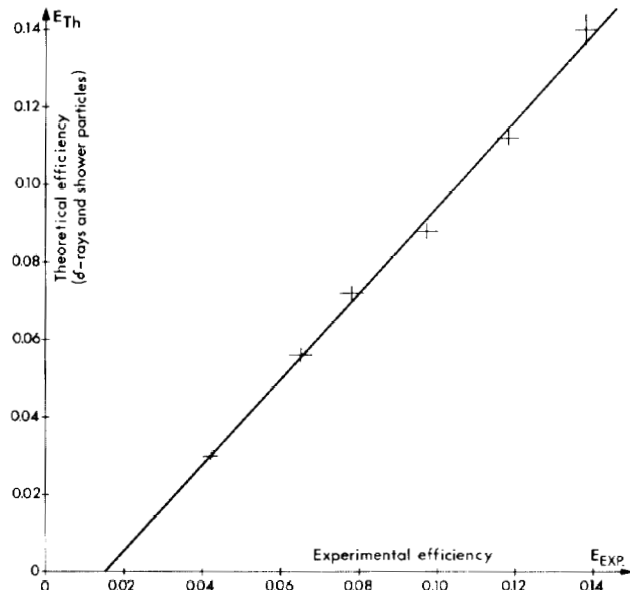

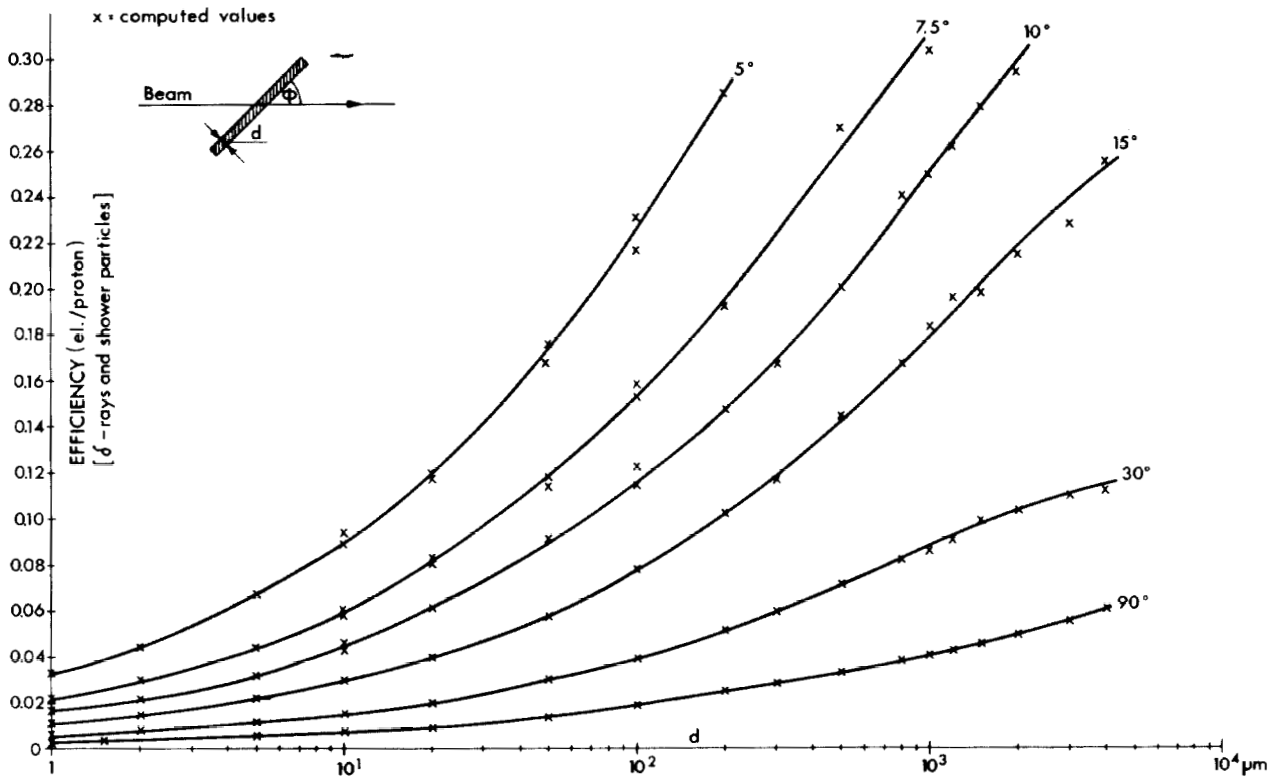Fig. 10. Computed values plotted against experimental efficiencies.

Fig. 9. Theoretical charge emission efficiency of inclined plates.